IGJ suppresses breast cancer growth and metastasis by inhibiting EMT via the NF-κB signaling pathway

MENGXUE WANG[1,2], YUSHEN WU[2,3], XUNJIA LI[4], MENG DAI[5] and SHENGWEI LI[1]

[1]Department of Hepatobiliary Surgery, The Second Affiliated Hospital of Chongqing Medical University, Chongqing 400010; [2]Chongqing Key Laboratory of Molecular Oncology and Epigenetics, and [3]Department of Oncology, The First Affiliated Hospital of Chongqing Medical University, Chongqing 400016; [4]Department of Nephrology, Chongqing Traditional Chinese Medicine Hospital, Chongqing 400013; [5]Department of Geriatric Oncology, Department of Palliative care, Chongqing University Cancer Hospital, Chongqing 400030, P.R. China

Received April 4, 2023; Accepted July 6, 2023

DOI: 10.3892/ijo.2023.5553

Abstract. Breast cancer metastasis is the primary cause of mortality of patients with breast cancer. The present study aimed to explore the role and underlying mechanisms of IGJ in the invasion and metastasis of breast cancer. The Cancer Genome Atlas database was utilized to analyze the differential gene expression profiles in patients with breast cancer with or without metastasis; the target gene, joining chain of multimeric IgA and IgM (JCHAIN, also known as IGJ, as referred to herein), with significant expression and with prognostic value was screened. The expression levels of IGJ in human breast cancer paired tissues and cell lines were detected using reverse transcription-quantitative PCR and western blot analysis. IGJ differential expression was detected in paired human breast cancer tissues using immunohistochemistry. The role of IGJ in breast cancer was verified using CCK-8, invasion and migration assays, and scratch tests *in vivo* and *in vitro*. Further exploration of the role and mechanism of IGJ in breast cancer was conducted through Gene Set Enrichment Analysis, Kyoto Encyclopedia of Genes and Genomes analysis, western blot analysis and immunofluorescence experiments. Through the analysis of gene expression profiles, it was found that IGJ was poorly expressed in patients with breast cancer with metastasis compared to patients with non-metastatic breast cancer. The overexpression of IGJ was associated with an improved distant metastasis-free survival and overall survival (OS). COX multivariate regression analysis demonstrated that IGJ was an independent prognostic factor for the OS and relapse-free survival of patients with breast cancer. In comparison to healthy breast cancer adjacent tissues and cell lines, IGJ was poorly expressed in breast cancer tissues and cell lines ($P<0.05$). Further analyses indicated that the overexpression of IGJ suppressed the proliferation, invasion and metastasis of breast cancer cells *in vivo* and *in vitro* by inhibiting the occurrence of epithelial-to-mesenchymal transition (EMT) and suppressing the nuclear translocation of p65. Finally, rescue experiments indicated that IGJ restricted the proliferation and metastasis of breast cancer cells by regulating the NF-κB signaling pathway. On the whole, the present study demonstrates that IGJ suppresses the invasion and metastasis of breast cancer by inhibiting both the occurrence of EMT and the NF-κB signaling pathway. These findings may provide novel biomarkers and potential therapeutic targets for the treatment of metastatic breast cancer.

Correspondence to: Professor Shengwei Li, Department of Hepatobiliary Surgery, The Second Affiliated Hospital of Chongqing Medical University, 76 Linjiang Road, Yuzhong, Chongqing 400010, P.R. China
E-mail: lishengwei11@163.com

Key words: IGJ, breast cancer, metastasis, epithelial-to-mesenchymal transition, NF-κB

Introduction

Breast cancer is the most prevalent malignancy affecting women worldwide, also ranking as the primary cause of cancer-related mortality among them (1). In spite of standardized comprehensive treatment for patients with early-stage breast cancer, ~20-30% of patients experience fatal distant recurrence and metastasis (2). The vast majority (~90%) of breast cancer-related deaths are due to distant metastasis (3). Therefore, breast cancer metastasis is the main reason affecting the prognosis of patients with breast cancer and the major challenge of breast cancer treatment. In primary tumors, epithelial-to-mesenchymal transition (EMT) plays a critical role in tumor cell invasion of the vascular system and the induction of proteases that degrade the extracellular matrix (4). EMT results in changes in cell surface structure, and leads to an increased invasive ability and a weakened adhesive ability. With EMT, the expression of the epithelial marker, E-cadherin, decreases, while that of the markers of interstitial cell phenotypes, N-cadherin and Vimentin, increases (5,6). Moreover, cells become spindle-shaped, intercellular adhesion weakens, and the movement and mobility of the cells are enhanced. Subsequently, the cells travel via the bloodstream to distant organs, gradually revert back to their original shape, and proliferate to form metastatic tumors (7).

The joining chain of multimeric IgA and IgM (JCHAIN, also known as IGJ, as referred to herein) gene is located on 4q13.3 and the translated protein is J chain (8). IGJ protein is composed of 159 amino acid residues with a molecular weight of ~15 kDa. Previous research has indicated that the J chain is involved in the formation of dimer IgA and multimer IgM, promoting their binding to secretory components and regulating the transport process of secretory immunoglobulins (dimer IgA and pentamer IgM) to realize exocytosis (9). The expression of the IGJ gene is accompanied by the differentiation and development of B- and T-lymphocytes, particularly after B cells differentiate into plasma cells, and the J chain is highly expressed with the production of immunoglobulin (10). In addition, IGJ protein can also be detected in dendritic cells, intestinal epithelial cells, endometrial cells and mammary epithelial cells (10). Given that the IGJ gene is expressed not only in immunoglobulin-secreting cells, but also in some non-immunoglobulin-secreting cells, the biological function of the J chain may extend beyond polymerized immunoglobulins (8,10). The expression of the IGJ gene is known to vary across various pathological conditions, with significant transcription changes in certain infectious diseases, autoimmune diseases and hematological tumors (11-13). In patients with acute B lymphoblastic leukemia, a high expression of IGJ indicates a poor disease-free survival and overall survival (OS) (13). The transcription level of IGJ in lung squamous cell carcinoma, adenocarcinoma tissues and gastric cancer has been found to be markedly lower than that in normal tissues (14,15). Some breast cancer prognostic prediction studies have found that IGJ exhibits a high accuracy in distinguishing breast cancer tissue from normal breast tissue, and that high levels of IGJ are associated with an improvised prognosis of patients with breast cancer, suggesting that IGJ may be utilized as a biomarker for breast cancer (16-19).

However, research on IGJ remains limited to a superficial level in malignant tumors, and its potential biological function and mechanisms underlying its involvement in malignant tumor occurrence and development remain unclear.

The present study aimed to identify novel therapeutic targets that can potentially inhibit breast cancer metastasis and increase the survival rates of patients. Through the investigation of genes that can promote or hinder tumor metastasis in breast cancer, the present study attempted to identify IGJ as the main target gene. It was hypothesized that IGJ may be an independent prognostic factor in breast cancer by inhibiting tumor metastasis and the EMT process. Verification assays were conducted to examine this hypothesis at the cellular level and to investigate whether the overexpression of IGJ is effective in suppressing the proliferation, migration, invasion and EMT process of breast cancer cell lines. Further experiments were conducted using nude mice to verify whether IGJ can inhibit breast cancer tumor growth.

Materials and methods

The Cancer Genome Atlas (TCGA) Chip data and Kaplan-Meier survival analysis. The TCGA high-throughput sequencing data for breast cancer were downloaded from the UCSC database (version 2015-02-24; available at https://genome.ucsc.edu/). To investigate the clinical relevance of IGJ, 991 patients with breast cancer from the TCGA database were included, whose RNA-seq data and clinical information were complete. The information included age, tumor size, lymph node metastasis, tumor size, tumor stage (TNM), estrogen receptor (ER), progesterone receptor (PR), human epidermal growth factor receptor 2 (HER2) and follow-up information. Kaplan-Meier analysis (http://kmplot.com/analysis/) was applied to analyze the association between IGJ expression and the prognosis of patients with breast cancer using the dataset from the study by Győrffy (20).

Differential gene screening. Differential gene analysis was performed for bone and lung metastasis. Statistical analyses were performed using R software 3.5.1 and DEseq, an R language package. An adjusted P-value <0.05 and a fold change >2 were considered to indicate statistically significant differences, and the difference in gene expression was regarded as significant between the experimental and the control groups.

Propensity score matching (PSM). To eliminate the difference in clinical baseline characteristics and selection bias between the metastatic group and the non-metastatic group, PSM was conducted for eight variables: Sex, age, tumor size, lymph node metastasis, ER, PR, HER2 and histological type. SPSS 25.0 software (IBM Corp.) was used to calculate individual PSM, randomly matching at a 1:1 ratio with a caliper value set to 0.05.

Clinical tissue samples. A total of 32 pairs of breast cancer tissues and adjacent normal tissues were collected from patients that underwent breast cancer resection at the First Affiliated Hospital of Chongqing Medical University (Chongqing, China) between 2014 and 2016. Moreover, 28 pairs of breast cancer tissues and normal tissues were collected from patients with breast cancer metastasis at follow-up. The collected tissues were used for reverse transcription-quantitative PCR (RT-qPCR) and immunohistochemistry (IHC), which were performed as described below. All specimens collected were preserved in liquid nitrogen. The collection and use of the tissues were approved by the Institutional Ethics Committee of the First Affiliated Hospital of Chongqing Medical University (approval no. 2017-012) and written informed consent was signed by the patients.

Cell lines. Healthy mammary epithelial cells (MCF-10A) and human breast cancer cells (T47D, YCC-B1, MDA-MB-231, MCF-7, SK-BR-3, ZR-75-1 and BT-549) were used in the present study. The YCC-B1 cell line was kindly provided as a gift from Professor Qian Tao at The Chinese University of Hong Kong (Hong Kong, SAR, China) and authenticated using short tandem repeat profiling. All other cell lines were obtained from the American Type Culture Collection (ATCC) cell bank (MCF-10A: cat. no. CRL-10317; TC7D: cat. no. HTB-133; MDA-MB-231: cat. no. HTB-26; MFC-7: cat. no. HTB-22; SK-BR-3: cat. no. HTB-30; ZR-75-1: cat. no. CRL-1500; BT-549: cat. no. HTB-122). The breast cancer cell lines were cultured in RPMI-1640 medium (Gibco; Thermo Fisher Scientific, Inc.) supplemented with 10% FBS (Gibco; Thermo Fisher Scientific, Inc.) and 1% penicillin-streptomycin. MCF-10A cells were cultured in DMEM/F12 (Gibco; Thermo Fisher Scientific, Inc.) containing 20 ng/ml EGF (Beijing

Table I. Primer sequences used in the present study.

Gene	Forward sequence (5' end to 3' end)	Reverse sequence (5' end to 3' end)
IGJ	TCCTGGCGGTTTTTATTAAGGC	AGTAATCCGGGCACACTTACAT
GAPDH	GGAGCGAGATCCCTCCAAAAT	GGCTGTTGTCATACTTCTCATGG

IGJ, joining chain of multimeric IgA and IgM (JCHAIN).

Solarbio Science & Technology Co., Ltd.), 0.5 μg/ml hydrocortisone, 10 μg/ml insulin, and 1% penicillin-streptomycin. All cells were in a cell incubator at 37˚C with 5% CO_2.

Cell transfection. The control plasmids (vector) and IGJ overexpression plasmids were obtained from Hanbio Biotechnology Co., Ltd. Lipofectamine 2000® (Invitrogen; Thermo Fisher Scientific, Inc.) was used to transfect the MDA-MB-231 and YCC-B1 cells. Subsequently, lipopolysaccharide (LPS; 10 μg/ml; cat. no. L8880, Beijing Solarbio Science & Technology Co., Ltd.) was added to the vector- and IGJ-treated cells, respectively. The cells were cultured for 48 h following transfection and then collected for use in subsequent experiments.

RNA isolation and RT-qPCR. As previously described (21), TRIzol® reagent (Thermo Fisher Scientific, Inc.) we used to extract total RNA following the manufacturer's instructions. The RT reaction was performed using the RT reagent kit (cat. no. RR047A; Takara Bio, Inc.), and the reaction conditions were 15 min at 37˚C and 5 sec at 85˚C. RT-qPCR (cat. no. RR820A; Takara Bio, Inc.) was performed to detect IGJ expression on 32 pairs of tissues using an ABI 7500 real-time PCR system (Applied Biosystems; Thermo Fisher Scientific, Inc.). The RT-qPCR reaction conditions were set as follows: 95˚C for 30 sec, 40 cycles at 95˚C for 3 sec, and 60˚C for 30 sec. The relative quantification of IGJ mRNA expression was normalized to the GAPDH expression level using the $2^{-\Delta\Delta Cq}$ method (22). The primer pairs used in the present study are listed in Table I.

Western blot analysis. Breast cancer cells were collected and lysed in a pre-cooled RIPA lysis buffer (Beyotime Institute of Biotechnology) for 20 min. The mixture was then centrifuged at high speed for 20 min at a minimal 17,383 x g, at 4˚C. Following centrifugation, the supernatant was collected and the protein concentration was quantified using a BCA protein assay kit (Wuhan Boster Biological Technology, Ltd.), and the protein sample was boiled and denatured at 100˚C. Electrophoresis separation was performed using 6 or 12% sodium dodecyl sulfate-polyacrylamide gel electrophoresis (SDS-PAGE) (Beyotime Institute of Biotechnology), and the protein was then transferred to a polyvinylidene fluoride (PVDF) membrane (MilliporeSigma). The membrane was blocked using 5% skim milk for 2 h at room temperature. Subsequently, diluted primary antibodies were added for protein culture overnight at 4˚C. Additionally, the membrane was washed three times using TBST, for 3 min each time. Subsequently, a diluted secondary antibody was added and the membrane was cultured at room temperature for 40 min, and the membrane was then rinsed with TBST three times, for 3 min each time. Protein bands were developed using an enhanced chemiluminescence (ECL) kit (Beyotime Institute of Biotechnology). GAPDH was used as an endogenous control. The primary antibodies used were the following: IGJ (1:1,000; cat. no. ab269855), β-actin (1:1,000; cat. no. ab8226) (both from Abcam), E-cadherin (1:1,000; cat. no. 14472), N-cadherin (1:1,000; cat. no. 13116), Vimentin (1:1,000; cat. no. 5741), Claudin-1 (1:1,000; cat. no. 13255), matrix metalloproteinase (MMP)9 (1:1,000; cat. no. 13667s), MMP7 (1:1,000; cat. no. 3801), p65 (1:1,000; cat. no. 8242), phosphorylated (p-)-p65 (Ser536; 1:1,000; cat. no. 3033), IκBα (1:1,000; cat. no. 4818), p-IκBα (Ser32; 1:1,000; cat. no. 5209), proliferating cell nuclear antigen (PCNA; 1:1,000; cat. no. 13110), and GAPDH (1:1,000; cat. no. 51332) (all from Cell Signaling Technology, Inc.). The secondary antibodies used were the following: Rabbit secondary antibody (1:4,000; cat. no. 7074) and mouse secondary antibody (1:4,000; cat. no. 7076) (both from Cell Signaling Technology, Inc.).

IHC. The procedures to conduct IHC followed the description of previous studies (21,23). The samples underwent formalin fixation and paraffin embedding before being sliced into 4-μm-thick sections and mounted onto glass slides. IHC was performed on the slides following deparaffinization and rehydration with xylene and a graded ethanol series for 0.5 h. Antigen retrieval was carried out by microwaving the samples in a sodium citrate-hydrochloric acid buffer solution at 95˚C for 20 min. To block endogenous horseradish peroxidase activity, the sections were then treated with 3% hydrogen peroxide and subsequently washed with phosphate-buffered saline (PBS) three times. Normal goat serum was applied to the sections as a blocking agent at 25˚C for 30 min. The anti-IGJ rabbit polyclonal antibody (1:100; cat. no. ab105229, Abcam) or Ki-67 mouse monoclonal antibody (1:1,000, cat. no. 9449, Cell Signaling Technology, Inc.) was added to the sections, followed by overnight incubation at 4˚C. Another round of PBS washing preceded incubation with goat anti-rabbit HRP secondary antibody (1:100; cat. no. SPN9001, OriGene Technologies, Inc.). After washing, the sections were treated with streptavidin-biotin-conjugated horseradish peroxidase (HRP), which was followed by visualization of signals using diaminobenzidine. Hematoxylin (cat. no. G1004, Wuhan Servicebio Technology Co., Ltd.) was applied to counterstain the sections at 25˚C for 1 min. A total of 28 pairs of tissues were subjected to IHC. IHC staining scores were used to indicate the intensity of staining: 0 represents no staining, 1 represents weak staining, 2 represents moderate staining, and

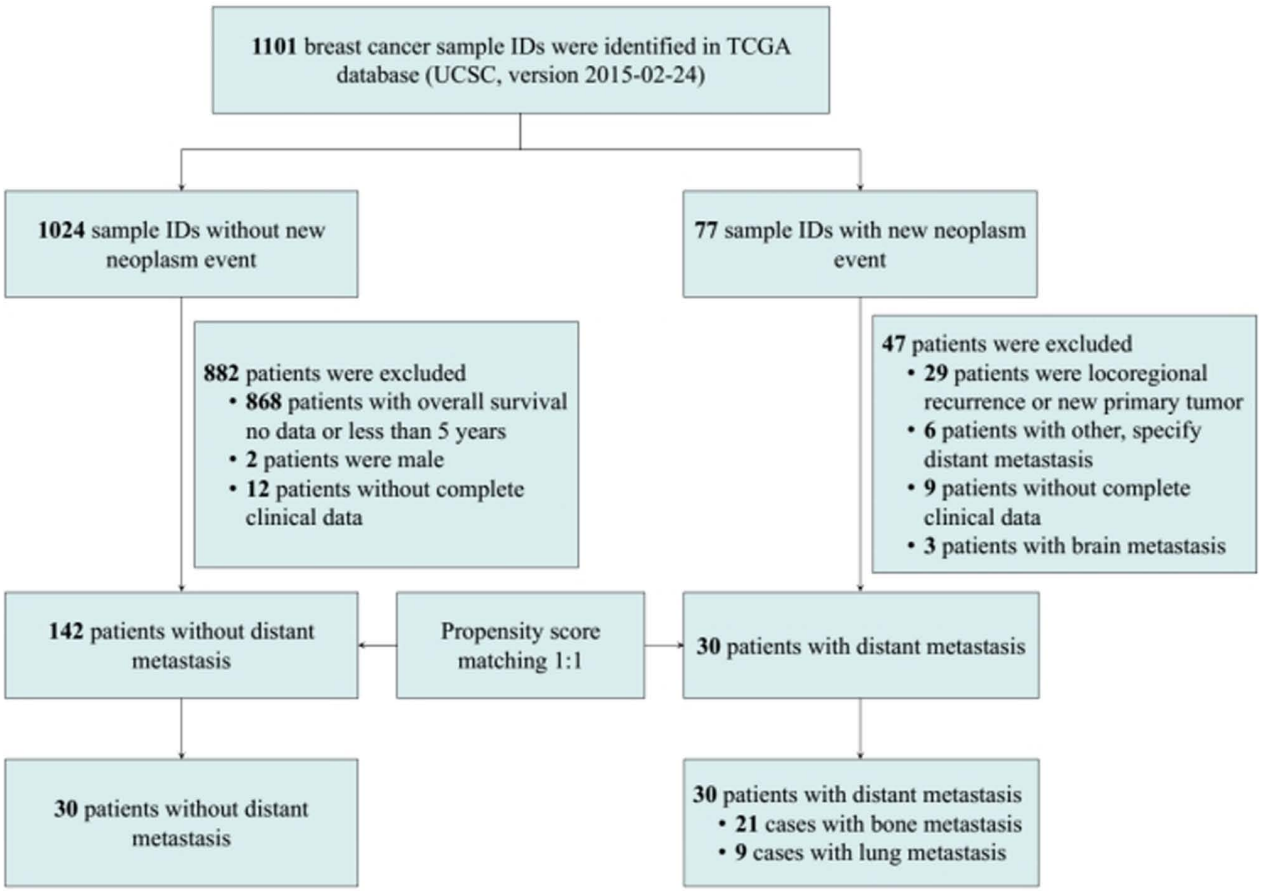

Figure 1. The Cancer Genome Atlas database screening process of patients with breast cancer.

3 represents strong staining. The scores for determining the proportion of positive tumor cells were 0, <5%; 1, 5-25%; 2, 26-50%; 3, 51-75%; and 4, >75%. The total score was calculated by multiplying the intensity scores and the percentage scores.

Immunofluorescence (IF) staining. The tumor tissue sections were boiled in citrate antigen retrieval solution (P0081, Beyotime Institute of Biotechnology) for 30 min. Subsequently, 0.5% Triton X-100 (cat. no. T8200, Beijing Solarbio Science & Technology Co., Ltd.) was added to the sections, followed by a 30-min incubation at room temperature. The sections were blocked with goat serum (cat. no. 16210064, Thermo Fisher Scientific, Inc.) at 25˚C for 30 min. The sections were then incubated overnight at 4˚C with E-cadherin (1:200; cat. no. 14472) or Vimentin (1:100; cat. no. 5741) antibodies (both from Cell Signaling Technology, Inc.). After washing with PBS, the sections were incubated at 25˚C in the dark for 1.5 h with Cy3 goat anti-rabbit IgG (1:50; cat. no. AS007) and FITC goat anti-rabbit IgG (1:50; cat. no. AS011) antibodies (both from ABclonal Technology Co., Ltd.). DAPI (cat. no. C1005, Beyotime Institute of Biotechnology) was then added to the sections and incubated in the dark for 5 min. The excess DAPI was washed away with PBS, and the sections were mounted using an anti-fade mounting medium (cat. no. P0126, Beyotime Institute of Biotechnology) to prevent fluorescence quenching. Finally, the sections were observed and photographed under an inverted fluorescent microscope [ICX41, Sunny Optical Technology (Group) Co Ltd.].

Cell Counting Kit-8 (CCK-8) assay. The cells in each group were collected in the logarithmic phase to prepare a single-cell suspension and cell density was adjusted after cell count calculation. The cells were then inoculated into 96-well plates ($1x10^3$ cells/well) and 10 μl CCK-8 reagent (Beyotime Institute of Biotechnology) was dripped into each well on days 1, 2 and 3, respectively. At 1 h following incubation at 37˚C, the absorbance of each well was measured at 450 nm wavelength using a xMark™ microplate spectrometer (Bench markPlus™ system, Bio-Rad Laboratories, Inc.). After 3 days, the cell proliferation curve was plotted based on the absorbance value.

Transwell assay. A Transwell chamber (MilliporeSigma) was used for the Transwell assays. The chamber for detecting cell invasion was covered with a layer of Matrigel (MilliporeSigma) and air-dried overnight. After the cells were resuspended in a serum-free medium at $1x10^5$ cells/ml, 200 μl of the breast cancer cell suspension were added to the upper chamber, and 600 μl medium containing 10% FBS was added to the lower chamber. Following 24 h of culture, the upper chamber was removed, and the cells were fixed with 4% paraformaldehyde at 25˚C for 20 min and stained with a 0.1% crystal violet solution (cat. no. DZ0055, Leagene Biotechnology) at 25˚C for 20 min. Additionally, after being washed with PBS three times, the cells remaining on the surface of the membrane were wiped off using a wet swab. The cells were subsequently counted under an inverted fluorescent microscope [ICX41, Sunny Optical Technology (Group) Co Ltd.].

Table II. Baseline characteristics of metastatic and non-metastatic patients following propensity score matching.

Characteristics	Cohort 1			Cohort 2		
	Non-metastasis	Bone metastasis	P-value	Non-metastasis	Lung metastasis	P-value
Sex/female, n	21	21	0.999	9	9	0.999
Age, median (range), years	54 (29-85)	56 (39-85)	NA	54 (42-62)	52 (49-69)	NA
Pathologic tumor size						
T1	6	4	0.80	0	2	NA
T2	7	10		8	6	
T3	7	6		1	1	
T4	1	1		0	0	
Pathologic lymph node status						
Negative	4	6	0.72	5	3	0.64
Positive	17	15		4	6	
ER status						
Negative	16	18	0.70	5	6	0.999
Positive	5	3		4	3	
PR status						
Negative	13	15	0.74	5	6	0.999
Positive	8	6		4	3	
HER2						
Negative	4	2	0.66	8	8	0.999
Positive	17	19		1	1	
Histological type						
IDC	15	12	0.61	6	6	0.55
ILD	3	4		0	1	
Other	3	5		3	2	

A Chi-squared test or Fisher's test was used to analyze the categorical data, and the non-parametric Mann-Whitney U rank sum test was used to analyze the continuous data. P<0.05 was considered to indicate a statistically significant difference. PMS, propensity score matching; IDC, infiltrating ductal carcinoma; ILD, infiltrating lobular carcinoma; ER, estrogen receptor; PR, progesterone receptor; HER2, human epidermal growth factor receptor 2; NA, not available.

Scratch test. The cells were seeded into six-well plates (5x10^6/well). When the plate was fully grown with cells, a straight line was marked using the tip of a sterile 200-μl pipette to create a direct scratch between the fused monolayer cells. The cells were then gently rinsed with a serum-free medium and scratched three times, and the scratches were observed and photographed under an inverted fluorescent microscope [0 h; ICX41, Sunny Optical Technology (Group) Co Ltd.]. Subsequently, the cells were cultured in a serum-free medium for 24 h, observed the scratches again, and photographed under an inverted fluorescent microscope [ICX41, Sunny Optical Technology (Group) Co Ltd.]. The healing of the scratches in each group indicated the migratory ability of the cells in each group.

Animal experiments. Healthy female BALB/c nude mice (4 weeks old, n=20) were purchased from Chongqing Ensiweier Biological Co., Ltd. The mice were raised in a pathogen-free environment with a temperature of 25˚C and a humidity range of 50 to 60%, and had free access to food and water. The nude mice were randomly divided into a control group and an IGJ overexpression group (n=10 per group). The MDA-MB-231 cells were subcutaneously injected into the right inguinal region or caudal vein as the control group. The tumor volume of the right inguinal region was measured, and the mouse body weights were assessed every 3 days for 5 consecutive weeks. After 30 days, 10 nude mice that had developed tumors in the right inguinal region were administered anesthesia by the intraperitoneal injection of 100 mg/kg ketamine and 5 mg/kg valium. Once it was confirmed that the anesthesia had taken effect, the mice were euthanized by an intraperitoneal injection of an overdose of pentobarbital sodium (200 mg/kg). Tumor tissues were then collected for weight and volume measurements. On day 33, the remaining 10 nude mice with tumors in the caudal vein were anesthetized by gas inhalation (2% isoflurane at 0.4 l/min gas flow) and photographed under a real-time imager (IVIS Lumina III, PerkinElmer, Inc.). Some tumor tissue samples were fixed in 4% paraformaldehyde at 25˚C for 24 h, and then stained with hematoxylin and eosin (H&E) at 25˚C for 5 min, while the remaining tissues were

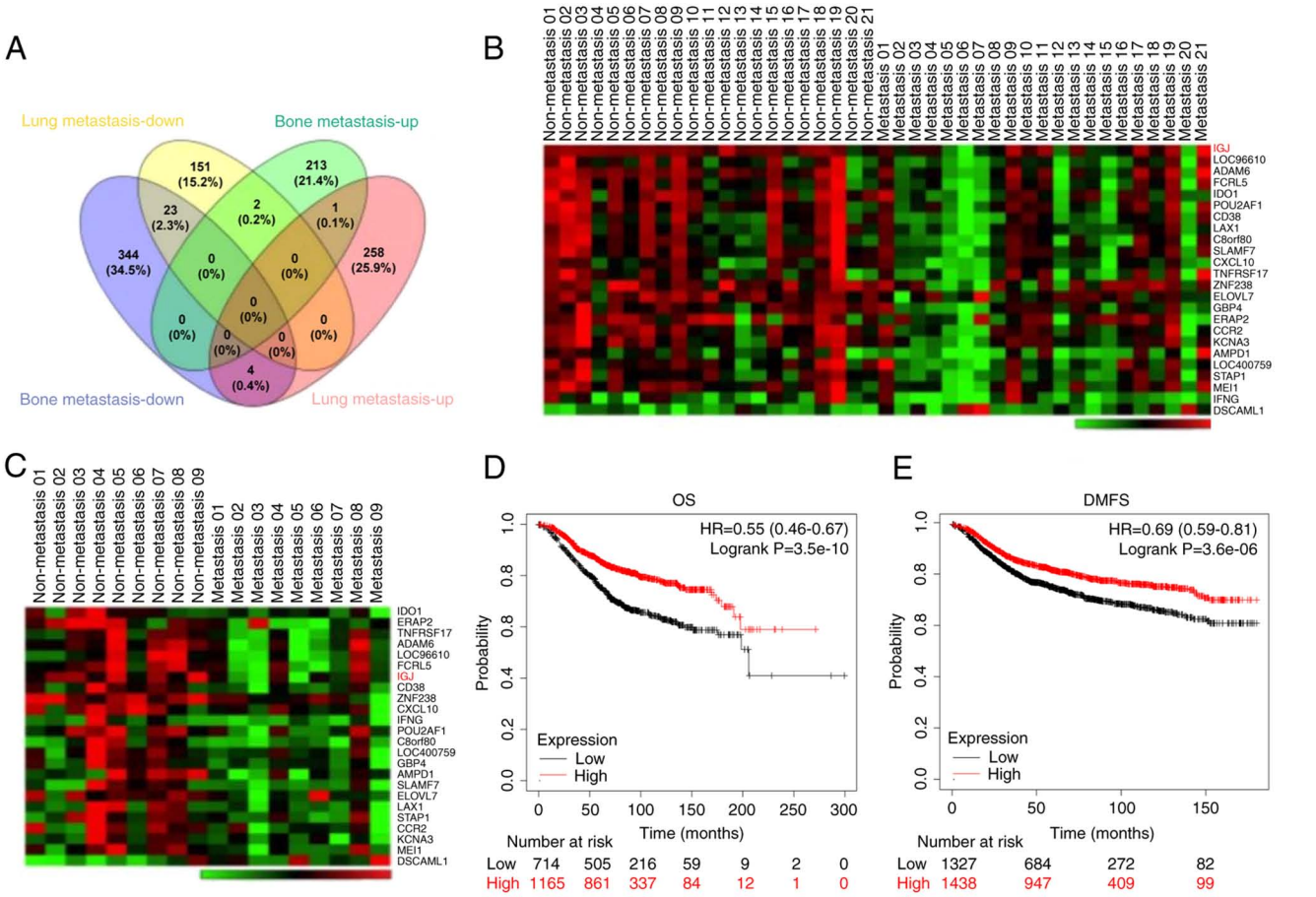

Figure 2. Screening of differential genes between the metastatic group and non-metastatic group in The Cancer Genome Atlas database. (A) Venn diagram depicting the simultaneous upregulation or downregulation of gene sets in the bone metastasis group and the lung metastasis group. (B and C) Heatmap depicted the differential genes in bone metastasis group and lung metastasis group. There were 587 differential genes in the bone metastasis group and 439 differential genes in the lung metastasis group; (D and E) Kaplan-Meier analysis of the results indicated that IGJ gene expression was related to the prognostic factors of patients with breast cancer; patients with a low IGJ expression had a poor prognosis; patients with a high IGJ expression had an improved prognosis. IGJ, joining chain of multimeric IgA and IgM (JCHAIN).

stored at -80˚C for further use. All experimental procedures were approved by the Animal Ethics Committee of Chongqing Medical University (approval no. 2022-K121).

Gene Set Enrichment Analysis (GSEA). GSEA (http://software.broadinstitute.org/gsea) was applied to analyze the association between IGJ expression and biological processes/Kyoto Encyclopedia of Genes and Genomes (KEGG) pathways according to the instructions of users. The microarray data set was GSE1456 and the gene set (c2 all.v6.0 symbols.gmt) for analyses was obtained from the Molecular Signatures Database (http://software.broadinstitute.org/gsea/msigdb/index.jsp). A false discovery rate (FDR) <0.25 and a P-value <0.05 were considered to indicate statistically significant differences.

Statistical analysis. All statistical analyses were performed using GraphPad Prism (version 8.0; Dotmatics) or SPSS software (Version 23.0; IBM Corp.). Cox regression analysis was used to estimate the association between IGJ expression and the prognosis [OS and distant metastasis-free survival (DMFS)] of patients with breast cancer. An unpaired Student's t-test was used to evaluate the difference between the two groups. One-way ANOVA with post hoc analysis using Tukey's test was used for comparisons between multiple groups. The Chi-squared test or Fisher's test was used to evaluate the significance between categorical data, and the non-parametric Mann-Whitney U test (Wilcoxon rank-sum test) was used to analyze the continuous data. A P-value <0.05 was considered significant to indicate a statistically significant difference.

Results

Screening of genes closely related to metastasis in patients with breast cancer. Through TCGA analysis, the high-throughput RNA sequencing data were obtained and 30 patients with non-metastatic breast cancer at diagnosis who had developed confirmed bone and lung metastasis during follow-up (21 with bone metastasis and 9 with lung metastasis) were screened. Subsequently, PSM was performed on these patients with breast cancer and those with breast cancer without metastasis at diagnosis and who developed no distant metastasis during the follow-up period (>5 years) according to clinical characteristics, such as age and tumor size (Fig. 1). No significant difference in was observed in the clinical characteristics between the two groups after matching (Table II). Subsequently, the differential genes between the metastatic and non-metastatic patients were

Table III. The association between the 24 differentially expressed genes and breast cancer prognosis.\

		DMFS			OS		
Gene symbol	Probe ID	HR	95% CI	Log-rank P-value	HR	95% CI	Log-rank P-value
Downregulated							
IGJ	212592_at	0.66	0.54-0.81	<0.001	0.56	0.45-0.69	<0.001
LOC96610	NA						
ADAM6	237909_at	0.58	0.40-0.83	0.003	0.72	0.52-1.00	0.048
FCRL5	224406_s_at	0.71	0.49-1.03	0.072	0.62	0.44-0.87	0.006
IDO1	210029_at	1.29	1.02-1.63	0.036	0.81	0.65-1.00	0.053
POU2AF1	205267_at	0.75	0.61-0.92	0.005	0.72	0.58-0.90	0.004
CD38	205692_s_at	0.75	0.60-0.95	0.015	0.73	0.58-0.92	0.007
LAX1	207734_at	0.74	0.60-0.90	0.003	0.69	0.54-0.87	0.001
C8orf80	NA						
SLAMF7	222838_at	0.64	0.44-0.95	0.025	0.53	0.37-0.75	<0.001
CXCL10	204533_at	1.34	1.09-1.65	0.005	0.76	0.60-0.98	0.030
TNFRSF17	206641_at	0.60	0.47-0.77	<0.001	0.67	0.54-0.83	<0.001
ZNF238	212774_at	0.66	0.54-0.80	<0.001	0.60	0.48-0.74	<0.001
ELOVL7	227180_at	1.25	0.89-1.77	0.200	0.82	0.60-1.12	0.220
GBP4	235175_at	0.68	0.48-0.97	0.031	0.52	0.38-0.71	<0.001
ERAP2	227462_at	0.74	0.53-1.03	0.075	0.67	0.48-0.93	0.017
CCR2	207794_at	0.78	0.62-0.97	0.028	0.64	0.52-0.79	<0.001
KCNA3	207237_at	0.8	0.63-1.01	0.064	0.83	0.64-1.07	0.142
AMPD1	206121_at	0.82	0.65-1.04	0.106	0.80	0.64-0.99	0.040
LOC400759	NA						
STAP1	1554343_a_at	0.67	0.46-0.97	0.032	0.63	0.45-0.87	0.005
MEI1	230011_at	0.66	0.43-0.99	0.043	0.58	0.43-0.80	<0.001
IFNG	210354_at	0.76	0.63-0.93	0.006	0.66	0.53-0.82	<0.001
Upregulated							
DSCAML1	234908_s_at	1.36	0.97-1.90	0.072	1.73	1.23-2.43	0.002

DMFS, distant metastasis free survival; OS, overall survival; HR, hazard ratio; NA, not available. P<0.05 was considered to indicate a statistically significant difference.

analyzed. Through differential gene analysis, there were 587 differential genes in the bone metastasis group and 439 differential genes in the lung metastasis group. When analyzing the differential genes between the metastatic and non-metastatic groups, the bone metastasis group and the lung metastasis group simultaneously included 23 downregulated genes and one upregulated gene (Fig. 2A-C). The Kaplan-Meier plotter database was employed to verify the association between the expression of these 24 genes and the prognosis of patients with breast cancer. Among the downregulated genes in the metastasis group, 13 genes (IGJ, ADAM6, POU2AF1, CD38, LAX1, SLAMF7, TNFRSF17, ZNF238, GBP4, CCR2, STAP1, MEI1 and IFNG) were associated with DMFS. Furthermore, the high expression of such genes indicated an improved OS (Table III). The high expression of IGJ was closely associated with an improved DMFS [hazard ratio (HR), 0.69; 95% confidence interval (CI), 0.59-0.81; P<0.001] and OS (HR, 0.55; 95% CI, 0.46-0.67, P<0.001) (Fig. 2D and E), and IGJ was determined as the target gene in the present study. The clinical association between IGJ and breast cancer in 991 patients with breast cancer was further analyzed in TCGA database; this revealed that IGJ expression was associated with age (P<0.001), lymph node metastasis (P<0.001) and ER status (P=0.027) (Table IV). Multivariate Cox regression analyses revealed that IGJ was an independent prognostic factor for OS (HR, 0.59; 95% CI, 0.421-0.866, P=0.007) and relapse-free survival (HR, 0.651; 95% CI, 0.461-0.837, P<0.001) in breast cancer (Table V).

Expression of IGJ in breast cancer. The present study first analyzed the expression of IGJ in breast cancer patients in TCGA database, which indicated that IGJ had the highest expression in adjacent tissues, but the lowest in metastatic breast cancer (Fig. 3A). In 114 cases of breast cancer in TCGA, the expression of IGJ in normal tissues was markedly higher than that in cancer tissues (Fig. 3B). Moreover, through the expression analyses of 32 pairs of normal breast tissues and paired cancer tissues collected from patients for the present study, the expression of IGJ in normal tissues was markedly higher than that in cancer tissues (Fig. 3C). IGJ mRNA and protein expression in the normal breast epithelial cell line,

Table IV. TCGA clinical correlation analysis of patients with breast cancer.

Characteristic	No. of cases	High (n)	Low (n)	P-value
Age, years				
<50	280	179	101	<0.001
≥50	711	368	343	
Tumor size				
T1	266	159	107	0.087
T2	577	309	268	
T3	119	68	51	
T4	29	11	18	
Lymph node metastasis				
Negative	474	226	248	<0.001
Positive	517	321	196	
TNM stage				
I	179	109	70	0.12
II	575	306	269	
III	225	128	97	
IV	12	4	8	
ER				
Positive	769	410	359	0.027
Negative	222	137	85	
PR				
Positive	672	367	305	0.592
Negative	319	180	139	
HER2				
Positive	202	107	95	0.476
Negative	789	440	349	
Triple-negative breast cancer				
Yes	166	100	66	0.152
No	825	447	378	

A Chi-squared test was used to analyze the categorical data, and the non-parametric Mann-Whitney U rank sum test was used to analyze the continuous data (tumor size and TMN stage). P<0.05 was considered to indicate a statistically significant difference. TCGA, The Cancer Genome Atlas; IGJ, joining chain of multimeric IgA and IgM (JCHAIN); ER, estrogen receptor, PR, progesterone receptor; HER2, human epidermal growth factor receptor 2.

MCF-10A, was markedly higher than that in breast cancer cells (Fig. 3D and E). Furthermore, the pathological section analysis of 28 pairs of breast cancer using IHC revealed that IGJ had the highest expression in normal tissues, whereas it had the lowest expression in breast cancer (Fig. 3F), suggesting that IGJ functions as a tumor suppressor gene in breast cancer.

Overexpression of IGJ inhibits the invasion and metastasis of breast cancer in vitro and in vivo. To explore the biological function of IGJ in breast cancer cells, the MDA-MB-231 and YCC-B1 cells were transfected with synthesized IGJ lentivirus or empty lentivirus vector and verification was conducted (Fig. S1). CCK-8 cell proliferation assay revealed that IGJ overexpression markedly inhibited the proliferation of breast cancer cells (Fig. 4A and C). In addition, Transwell assays revealed that the number of invasive or migratory breast cancer cells following the overexpression of IGJ was markedly reduced compared with the control group (Fig. 4B and D). The wound scratch tests also demonstrated that IGJ evidently inhibited the migration of breast cancer cells (Fig. 4E and F). Through subcutaneous tumorigenesis experiments in nude mice, it was found that compared with the vector group, the tumor size of the stable overexpression IGJ group was markedly smaller (Fig. 5A-D). The IHC detection of the expression of Ki-67 was conducted in the two groups with tumors (Fig. 5E). The *in vivo* imaging results revealed that the lung metastatic nodules of the nude mice in the IGJ overexpression group were markedly lower in number than those in the control group (Fig. 5F-H). These results indicated that IGJ inhibited the proliferation, invasion and metastasis of breast cancer cells *in vivo*.

IGJ inhibits EMT in breast cancer. Following GSEA analysis, it was found that the expression of IGJ in breast cancer was negatively associated with the occurrence of EMT (normalized

Table V. Univariate and multivariate COX regression analysis of IGJ in the TCGA cohort.

	OS						RFS					
	Univariate analysis			Multivariate analysis			Univariate analysis			Multivariate analysis		
Variant	HR	95% CI	P-value	HR	95% CI	P-value	HR	95% CI	P-value	HR	95% CI	P-value
Age, years (<50 vs. ≥50)	0.675	0.463-0.924	0.031	0.554	0.269-0.904	0.027	0.783	0.442-0.913	0.044	0.758	0.422-1.511	0.21
Tumor size (T1/T2 vs. T3/T4)	0.914	0.593-1.380	0.464				0.864	0.322-1.348	0.232			
Lymph node (N0 vs. N1/N2/N3)	0.476	0.345-0.863	0.001	0.673	0.414-1.031	0.873	0.698	0.343-1.321	0.317			
TNM stage (I/II vs. III/IV)	0.682	0.311-0.1.132	0.065				0.548	0.332-0.804	0.001	0.5497	0.347-0.843	0.011
ER (negative vs. positive)	1.274	0.883-1.614	0.174				1.126	0.532-1.895	0.743			
PR (negative vs. positive)	1.163	0.715-1.331	0.763				0.994	0.416-1.769	0.897			
HER2 (negative vs. positive)	1.48	0.945-2.317	0.086				1.203	0.678-2.875	0.512			
IGJ (high vs. low)	0.62	0.423-0.906	0.014	0.59	0.421-0.866	0.007	0.634	0.412-0.858	0.021	0.651	0.461-0.837	0.001

P<0.05 was considered to indicate a statistically significant difference. TCGA, The Cancer Genome Atlas; IGJ, joining chain of multimeric IgA and IgM (JCHAIN); ER, estrogen receptor; PR, progesterone receptor; HER2, human epidermal growth factor receptor 2; OS, overall survival; RFS, relapse-free survival; HR, hazard ratio; CI, confidence interval.

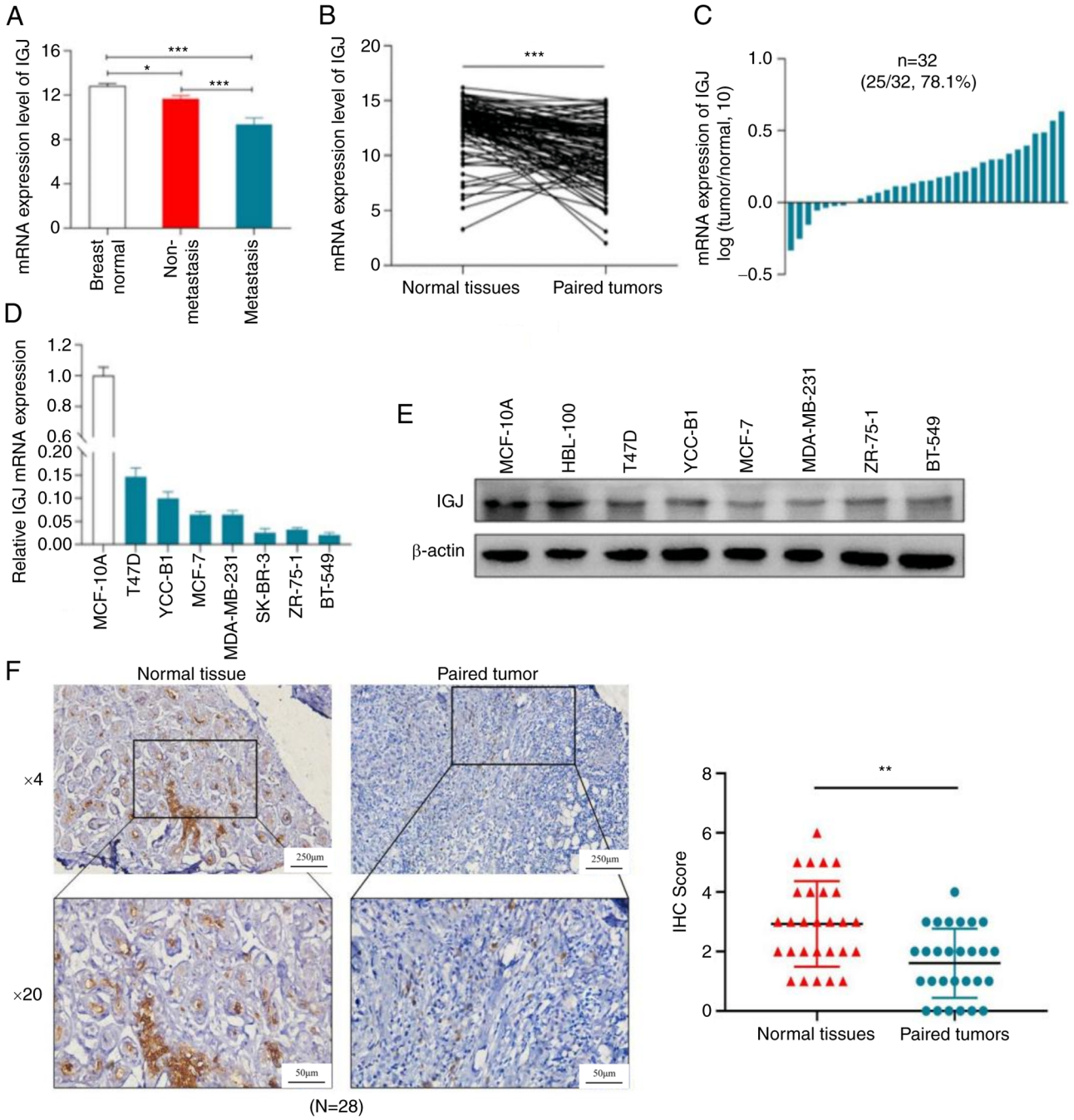

Figure 3. Expression of IGJ in breast cancer. (A) TCGA data indicated the highest expression of IGJ in normal breast tissues, and the lowest in metastatic breast cancer. A one-way ANOVA followed a post hoc test using Tukey's test was used for comparisons between groups (*P<0.05 and ***P<0.001). (B) The expression of 113 pairs of breast cancer and adjacent tissues in TCGA database; IGJ expression was higher in the adjacent tissues. (C) Reverse transcription-quantitative PCR detected the expression of 32 pairs of collected breast cancer tissue samples. (D) mRNA expression of IGJ in different breast cancer cell lines. (E) Protein expression of IGJ in different breast cancer cell lines. (F) Immunohistochemical detection of the 28 pairs of collected breast cancer tissue samples. An unpaired Student's t-test was used was used for comparisons between the two groups (**P<0.01). IGJ, joining chain of multimeric IgA and IgM (JCHAIN); TCGA, The Cancer Genome Atlas.

enrichment score, -2.31; Fig. 6A). Since GSEA analysis revealed that IGJ may be associated with EMT, the expression levels of the EMT markers, E-cadherin, N-cadherin, Clautin-1 and vimentin, were detected using western blot analysis. The results obtained confirmed that the overexpression of IGJ increased the expression of E-cadherin and claudin-1, while it decreased that of vimentin, N-cadherin, MMP9 and MMP7, thereby reversing EMT in breast cancer cells (Fig. 6B). Furthermore, additional evidence supporting the inhibitory effects of IGJ on EMT was provided by demonstrating that the overexpression of IGJ reversed EMT in breast cancer cells using IF staining (Fig. 6C).

IGJ regulates the NF-κB signaling pathway. IGJ was verified to be poorly expressed in breast cancer tissues and cells, and it inhibited the growth, invasion and metastasis of breast cancer, as well as the occurrence of EMT in breast cancer. These results suggested that IGJ functions as a tumor suppressor gene in

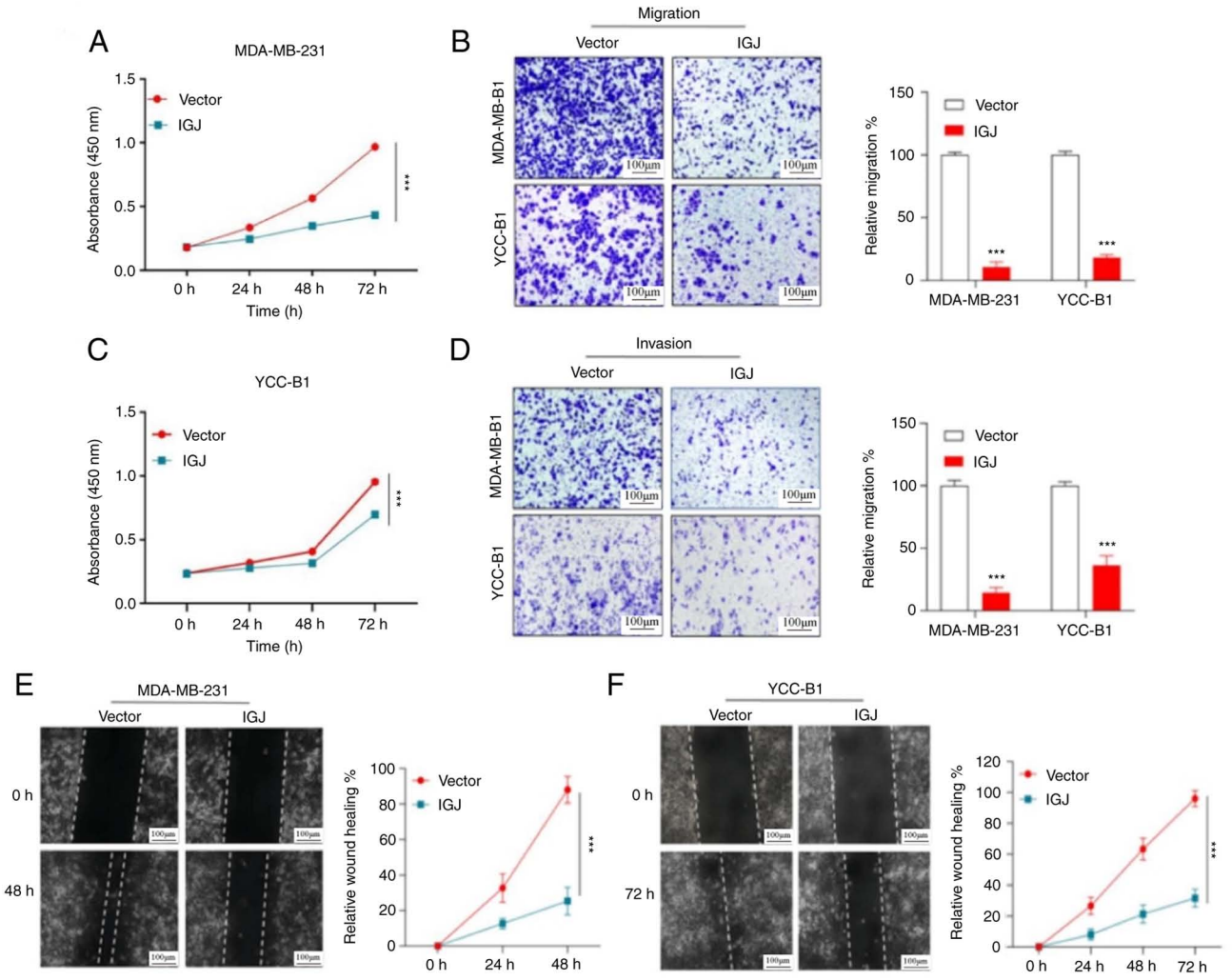

Figure 4. Effects of IGJ on the proliferation, invasion and migration of breast cancer cells. (A and C) CCK-8 assay indicated that IGJ inhibited cell proliferation. The results are expressed as the mean of three independent experiments ± SD (***P<0.001). (B and D) Transwell assay indicated that IGJ inhibited the migration and invasion of breast cancer cells. (E and F) Scratch assay revealed that IGJ inhibited the migration of breast cancer cells ***P<0.001. IGJ, joining chain of multimeric IgA and IgM (JCHAIN).

breast cancer; however, the underlying mechanisms remained unclear. Therefore, the mechanisms of IGJ in regulating breast cancer metastasis were further explored. To identify the possible IGJ-related pathways, KEGG analysis was conducted, indicating that the NF-κB signaling pathway may be one of the major enrichment pathways associated with IGJ (Fig. 7A). To determine the role of IGJ in the NF-κB pathway, the expression of the NF-κB pathway-related proteins, p65 and p-p65, were detected using western blot analysis. The overexpression of IGJ decreased the expression of p-p65 and p-IκBα, whereas it increased the expression of IκBα. However, the protein level of p65 was not markedly altered (Fig. 7B). To further reveal the mechanisms underlying the effects of IGJ on the NF-κB signaling pathway, nuclear and cytoplasmic proteins were extracted from IGJ-overexpressing and control cells to detect the expression of p65 using western blot analysis. The results indicated that the overexpression of IGJ markedly inhibited the nuclear accumulation of p65 in the MDA-MB-231 and YCC-B1 cells (Fig. 7C and D). Taken together, these findings indicate that IGJ inhibits the NF-κB signaling pathway by preventing the translocation of p65 into the nucleus.

IGJ inhibits the invasion and metastasis of breast cancer through the NF-κB signaling pathway. The present study demonstrated that IGJ inhibited the proliferation, invasion and metastasis of breast cancer cells, and IGJ was also found to inhibit the activation of the NF-κB signaling pathway. Since the NF-κB signaling pathway has been reported to be essential for the occurrence and development of tumors, it was hypothesized that IGJ inhibited the proliferation, invasion and metastasis of breast cancer cells by mediating the NF-κB pathway. Therefore, the NF-κB pathway agonist, LPS, we applied to conduct rescue experiments. It was found that the overexpression of IGJ markedly inhibited breast cancer cell proliferation following exposure to LPS; however, without LPS, cell proliferation was more markedly inhibited by IGJ overexpression; thus, LPS reduced the suppressive ability of IGJ on breast cancer (Fig. 8B and C). Similarly, Transwell assays revealed that LPS also reduced the ability of IGJ overexpression to inhibit the invasion and metastasis of breast cancer cells (Fig. 8A). These results suggested that IGJ played a role in breast cancer by regulating the NF-κB signaling pathway. Subsequently, the expression of various markers of

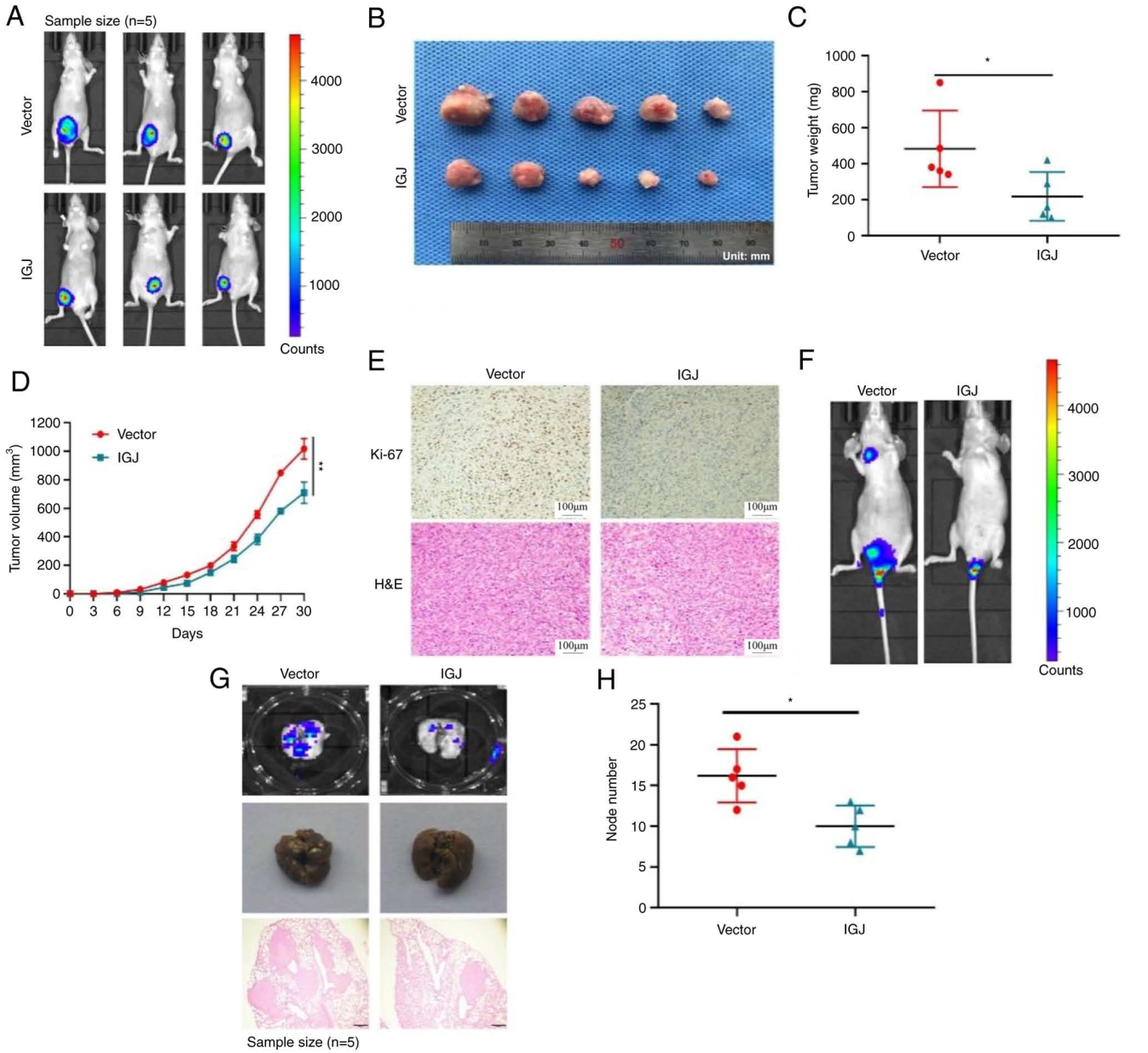

Figure 5. IGJ inhibits the proliferation and metastasis of breast cancer in nude mice. An unpaired Student's t-test was used was used for comparisons between the two groups (*P<0.05). (A-E) The growth of stable overexpression of IGJ breast cancer cells was markedly inhibited in nude mice (n=5 per group); (F-H) Overexpression of IGJ markedly inhibited the formation of metastatic pulmonary nodules in nude mice injected with breast cancer cells via caudal vein (n=5 per group). *P<0.05 and **P<0.01. IGJ, joining chain of multimeric IgA and IgM (JCHAIN).

EMT and protein molecules of the NF-κB signaling pathway was detected (Fig. 8D and E). These results indicated that the activation of the NF-κB signaling pathway was closely related to IGJ gene expression.

Discussion

Tumor metastasis is a complex, multi-step process involving several genes and biomolecules (24). At present, the understanding of the mechanisms underlying breast cancer metastasis is incomplete. A deeper insight into this process is crucial for improving the treatment efficacy in and prognosis of patients with clinical breast cancer. Current strategies for the treatment of breast cancer involve gene-specific, tissue-specific and genome-wide approaches to identify specific genes associated with specific breast cancer types, which can be applied to optimize the treatment of tumors for specific patients (25).

Given that the bone and lungs are the most common metastatic sites for breast cancer, the present study first collected data of breast cancer patients from TCGA database who initially reported no metastasis at diagnosis, but experienced it during follow-up. Moreover, non-metastatic breast cancer patients were matched with a series of clinical features similar to this group of patients. Through differential gene screening, a total of 24 genes with notable changes in expression were identified and IGJ was finally determined as the target gene of the present study via survival analysis. Further analysis revealed that IGJ was poorly expressed in breast cancer tissues and cells. The expression of IGJ was linked to age, lymph node metastasis and ER status. Multivariate COX regression analysis

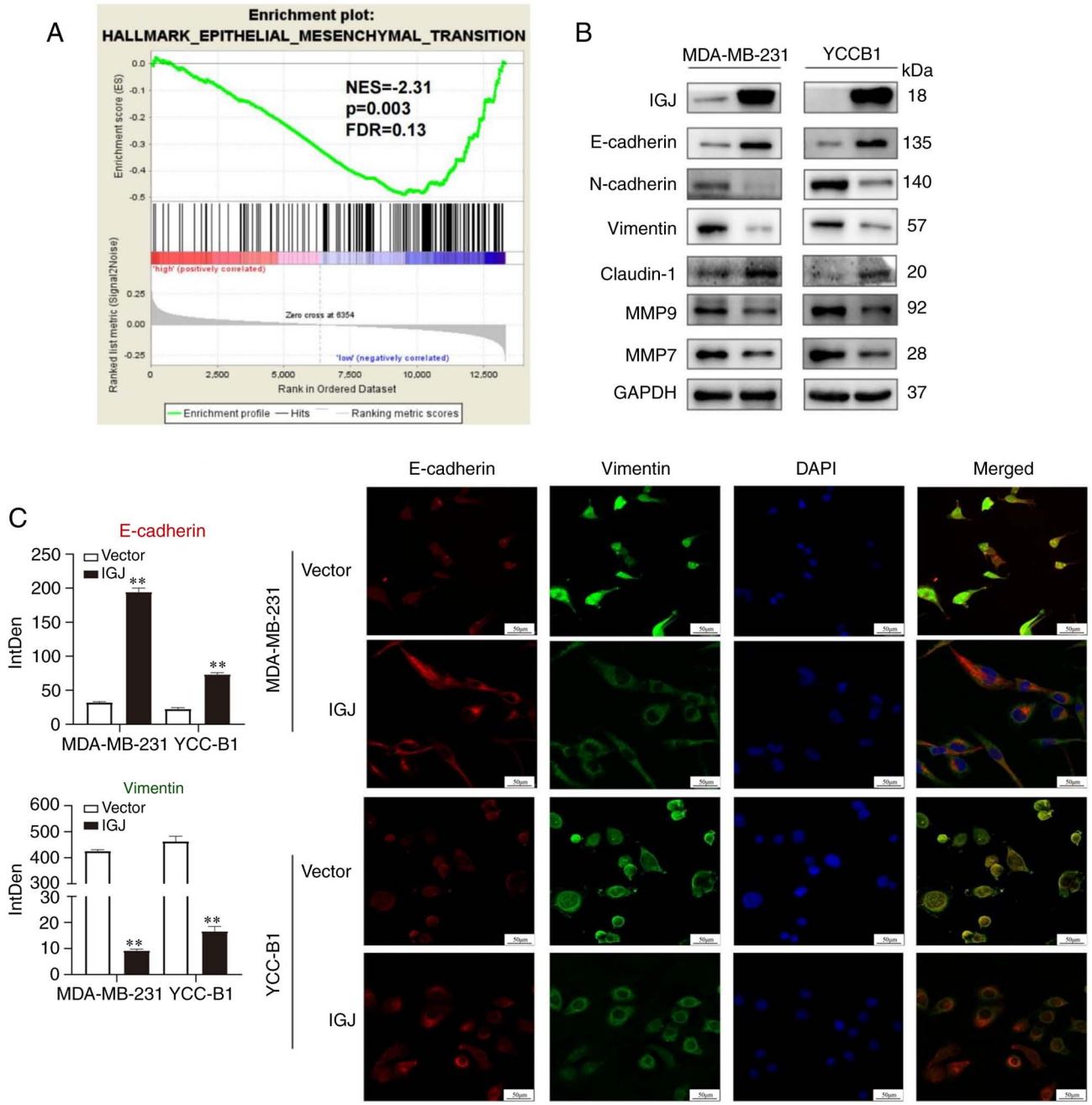

Figure 6. IGJ is involved in the regulation of the epithelial-to-mesenchymal transition process in breast cancer. (A) Bioinformatics data for predicting signaling pathways and biological processes involved in IGJ. (B and C) Western blot analysis and immunofluorescence staining were used to further verify the potential mechanism of IGJ affecting the biological behavior of breast cancer cells. **P<0.01. IGJ, joining chain of multimeric IgA and IgM (JCHAIN).

revealed that IGJ functioned as an independent prognostic factor for patients with breast cancer.

The present study also focused on the exploration of the biological role of IGJ in breast cancer. IGJ was revealed to inhibit the proliferation, invasion and metastasis of breast cancer *in vitro* and *in vivo*. Furthermore, a negative association was found between IGJ and EMT. A key change in promoting the migration and invasion of breast cancer cells has been recognized as the epithelial-EMT process (24,26). Over the past decade, multiple studies have reported the role of EMT in the invasion and metastasis of breast cancer (27-29). Epithelial cells are characterized by a complete intercellular interaction through adhesion molecules within tight junctions, adhesion junctions, desmosomes and gap junctions (30,31). However, due to various extracellular and tissue-specific EMT-induced signal stimuli, epithelial cells can upregulate EMT-induced transcription factors to coordinate all morphological, cellular and molecular changes during EMT, thereby promoting tumor metastasis (32). The tumor microenvironment plays a crucial role in determining the phenotype of epithelial cancer cells through a series of heterotypic cell signaling molecules. The Wnt, TGF-β and Notch signaling pathways have been identified as important components of the process of EMT (33). As research on the role of EMT in tumors continues to progress, its occurrence process and mechanisms have been gradually elucidated. In addition to the previously described classical

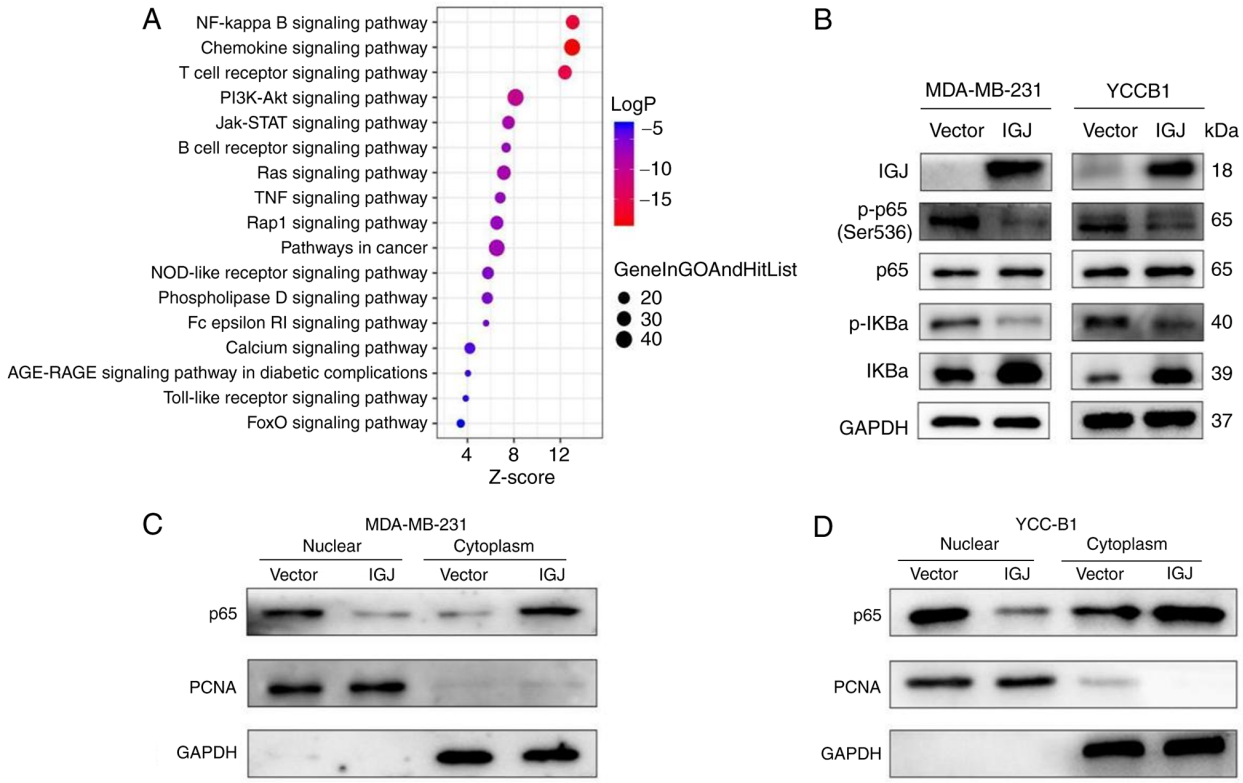

Figure 7. IGJ regulates the NF-κB signaling pathway in breast cancer. (A) Kyoto Encyclopedia of Genes and Genomes analysis indicated that IGJ mainly affects the NF-κB signaling pathway. (B) Western blot analysis detected the key molecules of the NF-κB signaling pathway. (C and D) Overexpression of IGJ inhibited the accumulation of p65 in the nuclear of MDA-MB-231 and YCC-B1 cells. IGJ, joining chain of multimeric IgA and IgM (JCHAIN); PCNA, proliferating cell nuclear antigen.

pathways, certain growth factors, including epidermal growth factor, insulin growth factor, hepatocyte growth factor, fibroblast growth factor and platelet-derived growth factor have also been found to trigger the EMT program (33-35). Moreover, it has been indicated that hypoxia-inducible factor 1α, inflammatory signals (NF-κB) and cytokines (IL-1β), and TNFα also induce the occurrence of EMT (36). Such pathways and cytokines act together in the occurrence of EMT in tumors. The occurrence and development of EMT in cancer cells may be regulated by numerous factors. Breast cancer cells may respond differently to signals from different pathways that cause EMT depending on their phenotypic status (35). Studies have indicated that triple-negative breast cancer cells can respond quickly to signals that induce EMT, particularly those transmitted by TGF-β (37,38). However, epithelial cancer cells of luminal breast cancer do not respond to the same EMT-induced signal and maintain the same state. The successful induction of EMT requires appropriate signaling and responsive target cells (39). Conversely, this suggests that the response of tumor cells to EMT-induced signals is applicable for the prediction of the future biological behavior of tumor cells at early stages of carcinogenesis (39,40). MMP is a type of protease, which has a number of biological functions in the development and progression of cancer (41). MMP9, also known as gelatinase B, plays a crucial role in extracellular matrix remodeling and protein cleavage, involving tumor invasion, metastasis, and the regulation of the tumor microenvironment (42). MMP9 is capable of breaking down collagen, and promoting migration, invasion and metastasis in basement membrane degradation (43). MMP7 is a secreted zinc and calcium dependent endopeptidase that is one of the most important downstream target genes of the Wnt/β-catenin signaling transduction. Its expression is associated with the poor prognosis of patients with breast cancer (43,44).

The present study discovered that IGJ was closely related to the NF-κB pathway and the expression of proteins p65 and p-p65 related to the NF-κB pathway was determined using western blot analysis. The results revealed that the overexpression of IGJ decreased the expression of p-p65 and p-IκBα, whereas it increased the expression of IκBα. The overexpression of IGJ markedly inhibited the nuclear accumulation of p65 in the MDA-MB-231 and YCC-B1 cells. NF-κB is one of the most complex transcription factors, consisting of five subunits (p50, p52, RelA, RelB and c-Rel), NF-κB inhibitor family (IκBs) and upstream activated kinase complex (IKKα, IKKβ and IKKγ)/NEMO (45,46). Normally, NF-κB forms heterodimers or homodimers isolated by IκB in the cytoplasm during the quiescent phase. Upon stimulation, IκB is phosphorylated by upstream kinases and is degraded through the ubiquitination-proteasome pathway, thereby releasing the active NF-κB dimer to regulate gene transcription inside the nucleus (47,48). Among several key factors in the progression of EMT, the NF-κB signaling pathway is a crucial factor in mediating the inflammatory process, and manipulating the occurrence and development of breast cancer (33). In this process, NF-κB may induce transcription factors SNAIL, TWIST and ZEB2 to enhance the occurrence of EMT and tumor metastasis (48-50). Several factors such as TGF-β1, ROS and TNF-α and hypoxia

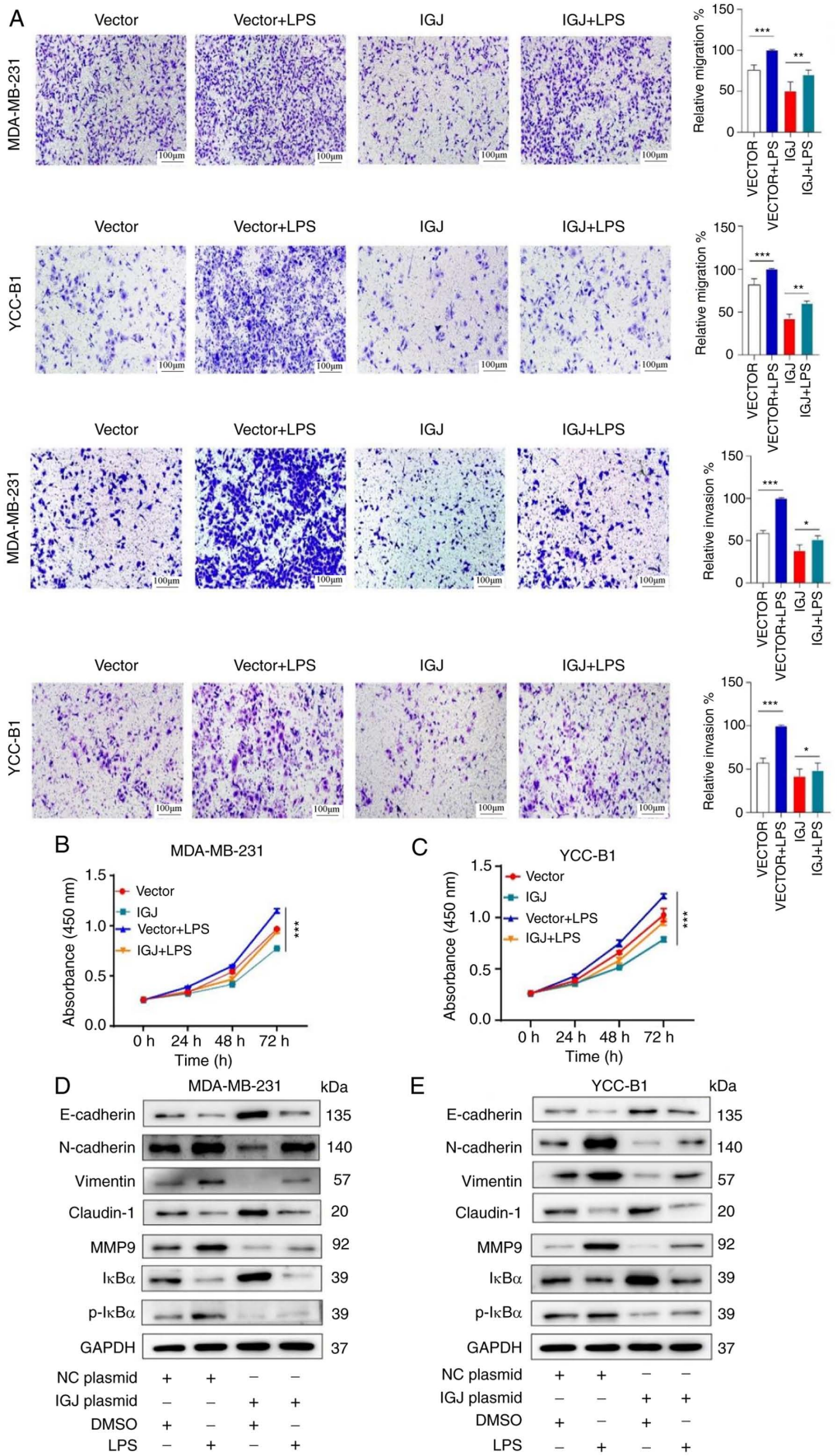

Figure 8. IGJ affects the proliferation and metastasis of breast cancer by regulating the NF-κB signaling pathway. A one-way ANOVA followed by a post hoc test Tukey's test was used for comparisons between groups (*P<0.05, **P<0.01 and ***P<0.001). (A) Transwell assay indicated a decreased ability of IGJ to inhibit the invasion and metastasis of breast cancer cells following the addition of LPS. (B and C) CCK-8 assay indicated that following the addition of LPS, IGJ inhibited the proliferation of breast cancer cells. (D and E) IGJ regulated the epithelial-to-mesenchymal transition process mainly through the NF-κB signaling pathway. IGJ, joining chain of multimeric IgA and IgM (JCHAIN); LPS, lipopolysaccharide; MMP, matrix metalloproteinase.

can also induce EMT *in vitro* and *in vivo*. EMT plays a role in AKT/GSK or NF-κB-mediated Snail expression, and promotes invasion and migration in various types of cancer, including breast, kidney and colon cancer (51,52). The loss of E-cadherin, a known adhesive cell surface protein expressed in epithelial cells, is the major feature of EMT (53). The key transcription factors, Snail and Slug, downregulate E-cadherin expression by binding to the E-box in the E-cadherin promoter, leading to the upregulation of MMP9 expression and the promotion of cell invasion (54).

Taken together, the present study demonstrated that IGJ suppressed the invasion and metastasis of breast cancer by inhibiting the occurrence of EMT and the NF-κB signaling pathway. These findings may provide novel biomarkers and therapeutic targets for the treatment of metastatic breast cancer.

While the present study provides valuable insight into breast cancer metastasis and the tole of IGJ, it is important to acknowledge certain limitations. Firstly, the present study was primarily based on bioinformatics analyses and *in vitro* experiments, which may not fully reflect the complex biological processes that occur in the human body. To confirm the therapeutic potential of IGJ as a target for breast cancer treatment, further *in vivo* experiments and clinical trials are warranted. Secondly, the sample size of the study was relatively small, and the tissue samples were all collected from a single center. The replication of these findings in larger and more diverse cohorts is crucial to ensure the generalizability of the results and their applicability to a broader population.

Acknowledgements

The authors would like to express their sincere gratitude to Professor Qian Tao at The Chinese University of Hong Kong (Hong Kong, SAR, China) for generously providing the YCC-B1 cell line used in the present study.

Funding

No funding was received.

Availability of data and materials

The datasets used and/or analyzed during the current study are available from the corresponding author on reasonable request.

Authors' contributions

MW and SL conceptualized the study. MW, YW, XL and MD carried out the formal analysis and investigations. MW wrote the original draft of the manuscript. MW, YW, and SL wrote, reviewed and edited the manuscript. MW, YW and SL confirm the authenticity of all the raw data. All authors have read and approved the final manuscript.

Ethics approval and consent to participate

The collection and use of the tissues in the present study were approved by the Institutional Ethics Committee of the First Affiliated Hospital of Chongqing Medical University and written informed consent was signed by the patients (approval no. 2017-012) and was bound by the Declaration of Helsinki. All experimental procedures were approved by the Animal Ethics Committee of Chongqing Medical University (approval no. 2022-K121).

Patient consent for publication

Not applicable.

Competing interests

The authors declare that they have no competing interests.

References

1. Bray F, Ferlay J, Soerjomataram I, Siegel RL, Torre LA and Jemal A: Global cancer statistics 2018: GLOBOCAN estimates of incidence and mortality worldwide for 36 cancers in 185 countries. CA Cancer J Clin 68: 394-424, 2018.
2. Early Breast Cancer Trialists' Collaborative Group (EBCTCG): Effects of chemotherapy and hormonal therapy for early breast cancer on recurrence and 15-year survival: An overview of the randomised trials. Lancet 365: 1687-1717, 2005.
3. Xie J, Ying YY, Xu B, Li Y, Zhang X and Li C: Metastasis pattern and prognosis of male breast cancer patients in US: A population-based study from SEER database. Ther Adv Med Oncol 11: 1758835919889003, 2019.
4. Kim MY: Breast cancer metastasis. Adv Exp Med Biol 1187: 183-204, 2021.
5. Das V, Bhattacharya S, Chikkaputtaiah C, Hazra S and Pal M: The basics of epithelial-mesenchymal transition (EMT): A study from a structure, dynamics, and functional perspective. J Cell Physiol 234: 14535-14555, 2019.
6. Thiery JP, Acloque H, Huang RY and Nieto MA: Epithelial-mesenchymal transitions in development and disease. Cell 139: 871-890, 2009.
7. Nieto MA: Epithelial-mesenchymal transitions in development and disease: Old views and new perspectives. Int J Dev Biol 53: 1541-1547, 2009.
8. Johansen FE, Braathen R and Brandtzaeg P: Role of J chain in secretory immunoglobulin formation. Scand J Immunol 52: 240-248, 2000.
9. Johansen FE, Braathen R and Brandtzaeg P: The J chain is essential for polymeric Ig receptor-mediated epithelial transport of IgA. J Immunol 167: 5185-5192, 2001.
10. Bertrand FE III, Billips LG, Gartland GL, Kubagawa H and Schroeder HW Jr: The J chain gene is transcribed during B and T lymphopoiesis in humans. J Immunol 156: 4240-4244, 1996.
11. Bjercke S and Brandtzaeg P: Glandular distribution of immunoglobulins, J chain, secretory component, and HLA-DR in the human endometrium throughout the menstrual cycle. Hum Reprod 8: 1420-1425, 1993.
12. Gui S, O'Neill WQ, Teknos TN and Pan Q: Plasma cell marker, immunoglobulin J polypeptide, predicts early disease-specific mortality in HPV+ HNSCC. J Immunother Cancer 9: e001259, 2021.
13. Cruz-Rodriguez N, Combita AL, Enciso LJ, Quijano SM, Pinzon PL, Lozano OC, Castillo JS, Li L, Bareño J, Cardozo C, *et al*: High expression of ID family and IGJ genes signature as predictor of low induction treatment response and worst survival in adult Hispanic patients with B-acute lymphoblastic leukemia. J Exp Clin Cancer Res 35: 64, 2016.
14. Slizhikova DK, Zinov'eva MV, Kuz'min DV, Snezhkov EB, Shakhparonov MI, Dmitriev RI, Antipova NV, Zavalova LL and Sverdlov ED: Decrease in expression of human J-chain in lung squamous cell cancer and adenocarcinoma. Mol Biol (Mosk) 41: 659-665, 2007 (In Russian).
15. Jiang B, Li S, Jiang Z and Shao P: Gastric cancer associated genes identified by an integrative analysis of gene expression data. Biomed Res Int 2017: 7259097, 2017.
16. Larsson C, Ehinger A, Winslow S, Leandersson K, Klintman M, Dahl L, Vallon-Christersson J, Häkkinen J, Hegardt C, Manjer J, *et al*: Prognostic implications of the expression levels of different immunoglobulin heavy chain-encoding RNAs in early breast cancer. NPJ Breast Cancer 6: 28, 2020.

17. Zhong Z, Jiang W, Zhang J, Li Z and Fan F: Identification and validation of a novel 16-gene prognostic signature for patients with breast cancer. Sci Rep 12: 12349, 2022.
18. Junjun S, Yangyanqiu W, Jing Z, Jie P, Jian C, Yuefen P and Shuwen H: Prognostic model based on six PD-1 expression and immune infiltration-associated genes predicts survival in breast cancer. Breast Cancer 29: 666-676, 2022.
19. Wang Y, Zhu M, Guo F, Song Y, Fan X and Qin G: Identification of tumor microenvironment-related prognostic biomarkers in luminal breast cancer. Front Genet 11: 555865, 2020.
20. Győrffy B: Survival analysis across the entire transcriptome identifies biomarkers with the highest prognostic power in breast cancer. Comput Struct Biotechnol J 19: 4101-4109, 2021.
21. Wang M, Dai M, Wu YS, Yi Z, Li Y and Ren G: Immunoglobulin superfamily member 10 is a novel prognostic biomarker for breast cancer. PeerJ 8: e10128, 2020.
22. Livak KJ and Schmittgen TD: Analysis of relative gene expression data using real-time quantitative PCR and the 2(-Delta Delta C(T)) method. Methods 25: 402-408, 2001.
23. Li Y, Huang J, Zeng B, Yang D, Sun J, Yin X, Lu M, Qiu Z, Peng W, Xiang T, *et al*: PSMD2 regulates breast cancer cell proliferation and cell cycle progression by modulating p21 and p27 proteasomal degradation. Cancer Lett 430: 109-122, 2018.
24. Kozłowski J, Kozłowska A and Kocki J: Breast cancer metastasis-insight into selected molecular mechanisms of the phenomenon. Postepy Hig Med Dosw (Online) 69: 447-451, 2015.
25. Stark AM, Tongers K, Maass N, Mehdorn HM and Held-Feindt J: Reduced metastasis-suppressor gene mRNA-expression in breast cancer brain metastases. J Cancer Res Clin Oncol 131: 191-198, 2005.
26. Chakrabarti R, Hwang J, Blanco MA, Wei Y, Lukačišin M, Romano RA, Smalley K, Liu S, Yang Q, Ibrahim T, *et al*: Elf5 inhibits the epithelial-mesenchymal transition in mammary gland development and breast cancer metastasis by transcriptionally repressing Snail2. Nat Cell Biol 14: 1212-1222, 2012.
27. Li CJ, Chu PY, Yiang GT and Wu MY: The molecular mechanism of epithelial-mesenchymal transition for breast carcinogenesis. Biomolecules 9: 476, 2019.
28. Yeung KT and Yang J: Epithelial-mesenchymal transition in tumor metastasis. Mol Oncol 11: 28-39, 2017.
29. Park M, Kim D, Ko S, Kim A, Mo K and Yoon H: Breast cancer metastasis: Mechanisms and therapeutic implications. Int J Mol Sci 23: 6806, 2022.
30. Karamanou K, Franchi M, Vynios D and Brézillon S: Epithelial-to-mesenchymal transition and invadopodia markers in breast cancer: Lumican a key regulator. Semin Cancer Biol 62: 125-133, 2020.
31. Wang H, Guo S, Kim SJ, Shao F, Ho JWK, Wong KU, Miao Z, Hao D, Zhao M, Xu J, *et al*: Cisplatin prevents breast cancer metastasis through blocking early EMT and retards cancer growth together with paclitaxel. Theranostics 11: 2442-2459, 2021.
32. Lüönd F, Sugiyama N, Bill R, Bornes L, Hager C, Tang F, Santacroce N, Beisel C, Ivanek R, Bürglin T, *et al*: Distinct contributions of partial and full EMT to breast cancer malignancy. Dev Cell 56: 3203-3221.e11, 2021.
33. Chaffer CL, Juan BP, Lim E and Weinberg RA: EMT, cell plasticity and metastasis. Cancer Metastasis Rev 35: 645-654, 2016.
34. Lamouille S, Xu J and Derynck R: Molecular mechanisms of epithelial-mesenchymal transition. Nat Rev Mol Cell Biol 15: 178-196, 2014.
35. Ho GY, Kyran EL, Bedo J, Wakefield MJ, Ennis DP, Mirza HB, Vandenberg CJ, Lieschke E, Farrell A, Hadla A, *et al*: Epithelial-to-mesenchymal transition supports ovarian carcinosarcoma tumorigenesis and confers sensitivity to microtubule-targeting with eribulin. Cancer Res 83: 4457-4473, 2022.
36. Hasmim M, Xiao M, Van Moer K, Kumar A, Oniga A, Mittelbronn M, Duhem C, Chammout A, Berchem G, Thiery JP, *et al*: SNAI1-dependent upregulation of CD73 increases extracellular adenosine release to mediate immune suppression in TNBC. Front Immunol 13: 982821, 2022.
37. Smith BN and Bhowmick NA: Role of EMT in metastasis and therapy resistance. J Clin Med 5: 17, 2016.
38. Huang Y, Hong W and Wei X: The molecular mechanisms and therapeutic strategies of EMT in tumor progression and metastasis. J Hematol Oncol 15: 129, 2022.
39. Chaffer CL, Marjanovic ND, Lee T, Bell G, Kleer CG, Reinhardt F, D'Alessio AC, Young RA and Weinberg RA: Poised chromatin at the ZEB1 promoter enables breast cancer cell plasticity and enhances tumorigenicity. Cell 154: 61-74, 2013.
40. Hashemi M, Moosavi MS, Abed HM, Dehghani M, Aalipour M, Ali Heydari E, Behroozaghdam M, Entezari M, Salimimoghadam S, Gunduz ES, *et al*: Long non-coding RNA (lncRNA) H19 in human cancer: From proliferation and metastasis to therapy. Pharmacol Res 184: 106418, 2022.
41. Gialeli C, Theocharis AD and Karamanos NK: Roles of matrix metalloproteinases in cancer progression and their pharmacological targeting. FEBS J 278: 16-27, 2011.
42. Mehner C, Hockla A, Miller E, Ran S, Radisky DS and Radisky ES: Tumor cell-produced matrix metalloproteinase 9 (MMP-9) drives malignant progression and metastasis of basal-like triple negative breast cancer. Oncotarget 5: 2736-2749, 2014.
43. Nagase H, Visse R and Murphy G: Structure and function of matrix metalloproteinases and TIMPs. Cardiovasc Res 69: 562-573, 2006.
44. Jabłońska-Trypuć A, Matejczyk M and Rosochacki S: Matrix metalloproteinases (MMPs), the main extracellular matrix (ECM) enzymes in collagen degradation, as a target for anticancer drugs. J Enzyme Inhib Med Chem 31 (sup1): S177-S183, 2016.
45. Vallabhapurapu S and Karin M: Regulation and function of NF-kappaB transcription factors in the immune system. Annu Rev Immunol 27: 693-733, 2009.
46. Muaddi H, Majumder M, Peidis P, Papadakis AI, Holcik M, Scheuner D, Kaufman RJ, Hatzoglou M and Koromilas AE: Phosphorylation of eIF2α at serine 51 is an important determinant of cell survival and adaptation to glucose deficiency. Mol Biol Cell 21: 3220-3231, 2010.
47. Pal S, Bhattacharjee A, Ali A, Mandal NC, Mandal SC and Pal M: Chronic inflammation and cancer: potential chemoprevention through nuclear factor kappa B and p53 mutual antagonism. J Inflamm (Lond) 11: 23, 2014.
48. Julien S, Puig I, Caretti E, Bonaventure J, Nelles L, van Roy F, Dargemont C, de Herreros AG, Bellacosa A and Larue L: Activation of NF-kappaB by Akt upregulates Snail expression and induces epithelium mesenchyme transition. Oncogene 26: 7445-7456, 2007.
49. Tsubaki M, Komai M, Fujimoto SI, Itoh T, Imano M, Sakamoto K, Shimaoka H, Takeda T, Ogawa N, Mashimo K, *et al*: Activation of NF-κB by the RANKL/RANK system up-regulates snail and twist expressions and induces epithelial-to-mesenchymal transition in mammary tumor cell lines. J Exp Clin Cancer Res 32: 62, 2013.
50. Katoh M and Katoh M: Integrative genomic analyses of ZEB2: Transcriptional regulation of ZEB2 based on SMADs, ETS1, HIF1alpha, POU/OCT, and NF-kappaB. Int J Oncol 34: 1737-1742, 2009.
51. Li CW, Xia W, Huo L, Lim SO, Wu Y, Hsu JL, Chao CH, Yamaguchi H, Yang NK, Ding Q, *et al*: Epithelial-mesenchymal transition induced by TNF-α requires NF-κB-mediated transcriptional upregulation of Twist1. Cancer Res 72: 1290-1300, 2012.
52. Wu Y, Deng J, Rychahou PG, Qiu S, Evers BM and Zhou BP: Stabilization of snail by NF-kappaB is required for inflammation-induced cell migration and invasion. Cancer Cell 15: 416-428, 2009.
53. Wang H, Wang HS, Zhou BH, Li CL, Zhang F, Wang XF, Zhang G, Bu XZ, Cai SH and Du J: Epithelial-mesenchymal transition (EMT) induced by TNF-α requires AKT/GSK-3β-mediated stabilization of snail in colorectal cancer. PLoS One 8: e56664, 2013.
54. Dongre A and Weinberg RA: New insights into the mechanisms of epithelial-mesenchymal transition and implications for cancer. Nat Rev Mol Cell Biol 20: 69-84, 2019.